



**HAL**  
open science

## The transitioning feature between uncooked and cooked cowpea seeds studied by the mechanical compression test

Ekoué Teko, Eलो Osseyi, Claire D. Munialo, Komla Ako

### ► To cite this version:

Ekoué Teko, Eलो Osseyi, Claire D. Munialo, Komla Ako. The transitioning feature between uncooked and cooked cowpea seeds studied by the mechanical compression test. *Journal of Food Engineering*, 2021, 292, pp.110368 -. 10.1016/j.jfoodeng.2020.110368 . hal-03492866

**HAL Id: hal-03492866**

**<https://hal.science/hal-03492866v1>**

Submitted on 17 Oct 2022

**HAL** is a multi-disciplinary open access archive for the deposit and dissemination of scientific research documents, whether they are published or not. The documents may come from teaching and research institutions in France or abroad, or from public or private research centers.

L'archive ouverte pluridisciplinaire **HAL**, est destinée au dépôt et à la diffusion de documents scientifiques de niveau recherche, publiés ou non, émanant des établissements d'enseignement et de recherche français ou étrangers, des laboratoires publics ou privés.



Distributed under a Creative Commons Attribution - NonCommercial 4.0 International License

1 **The transitioning feature between uncooked and cooked cowpea seeds**  
2 **studied by the mechanical compression test**

3 **Authors and affiliations:**

4 TEKO Ekoué<sup>a</sup>, OSSEYI Elolo<sup>a</sup>, MUNIALO D. Claire<sup>b</sup>, AKO Komla<sup>\*c,d</sup>

5 a) Département des sciences des Aliments et Technologie Agroalimentaire (SATA), ESTBA-  
6 UL B.P.1515-Lomé (TOGO)

7 b) School of Life Sciences, Coventry University, Priory Street, Coventry, CV1 5FB UK

8 c) Univ. Grenoble Alpes, LRP, F-38000 Grenoble, France

9 d) CNRS, LRP, F-38000 Grenoble, France

10 **\*Corresponding author:** *komla.ako@univ-grenoble-alpes.fr ; akokomla@hotmail.com*

11 **Abstract:**

12 Mechanical tests can allow for the mimicking of the textural attributes of foods as perceived  
13 by humans. Here we report on the use of the mechanical compression test to study the  
14 reactions underlying the cooking of the cowpea seeds (beans) until doneness. The creep test  
15 was applied to deal with the time-dependence of the strain,  $\epsilon(t)$ , at a constant force and to  
16 derive the elastic,  $K_e$  and viscosity,  $K_v$  indices for the different heating times. The results,  $\epsilon(t)$ ,  
17 were fitted using mostly a stretched exponential with a linear asymptotic(time) function. The  
18 flow rate ( $\omega$ ) and the strain ( $\epsilon$ ) are the constants of the asymptotic function. Both  
19 viscoelasticity indices decreased strongly before the first 30 min (from 562 N to 14 N for  $K_e$   
20 and from  $5.4 \times 10^6$  N.s to  $0.11 \times 10^6$  N.s for  $K_v$ ), but from 30 to 75 min  $\pm$  3 min,  $K_e$  remained  
21 almost constant ( $\sim$ 14 N) while  $K_v$  increases (from  $0.11 \times 10^6$  to  $0.24 \times 10^6$  N.s). Both  
22 viscoelasticity indices decreased strongly again after 75 min  $\pm$  3 min (from 14 N and  $0.24 \times 10^6$   
23 N.s for  $K_e$  and  $K_v$  respectively). The heating time-dependence of the viscoelasticity indices

24 clearly reflects the cowpeas beans transitioning to the cooked state and this may be correlated  
25 directly to the kinetic of water absorption, starch gelatinization and protein denaturation. This  
26 would correlate not only to the cooking time but also to the nutrient quantity balance. The  
27 results from this study shows that the samples mechanical properties with the simmering time  
28 correlate with the cooking reaction transitioning.

29 ***Keywords: Cowpeas; texture; gelatinization; yielding; stiffness; cooking time***

30

## 31 **1. Introduction**

32 Cooking is a practice that requires knowledge and technical skills for controlling the food  
33 transformation particularly its texture and flavor until the food is considered as ready for  
34 consumption. Many vegetables such as fruits, legumes, roots and seeds, are edible uncooked  
35 or cooked. Therefore, it is difficult to know fundamentally whether those vegetables are  
36 cooked with only the processing time and texture (Kouemene et al., 2013). The appreciation  
37 of the food in terms of cooked or uncooked depends on an individual's sensory perception and  
38 expectation as the vocabulary can vary with the people's level of training, culture and their  
39 own eating habits. However, at any rate the applied cooking method must provide energy to  
40 the food sufficiently to activate physical and/or chemical reactions of the food's elementary  
41 compounds (Coffigniez et al., 2018). Thus, food is cooked when the reactions underlying the  
42 cooking of the foods are done (Coffigniez et al., 2018). Thermodynamic, i.e. the states and  
43 transition states of the food compounds, with kinetics, i.e. the speed of the reactions, drive the  
44 cooking process (Coffigniez et al., 2018; Phillips et al., 1988). The difficulty is to find the  
45 operational textural variables in phase with both the thermodynamic and kinetic variables of  
46 the reactions by which food engineers can tell quantitatively the onset and the end of the  
47 cooking reaction processes, or at least can identify the transitioning period between uncooked  
48 and cooked state (Kouemene et al., 2013).

49 In this work, the transitioning of the cowpea seeds to the cooked state was investigated.  
50 Cowpea (*Vigna unguiculata*) is a legume of multiple variety seeds which consists of a testa  
51 with a hilum and micropyle, two cotyledons and an embryonic axis (Swanson et al., 1985).  
52 The bean constitutes of moisture (5 - 15 %), proteins (20 - 26 %), carbohydrates, starch (40 -  
53 70 %), fibre (3 - 5 %), and fat (1 - 3 %) (Adebooye and Singh, 2007; Coffigniez et al., 2019;  
54 Khattab et al., 2009). Cowpea bean contains B-vitamins namely, thiamine (~0.9 %) and

55 riboflavin (~0.15 %) (Edijala, 1980; Phillips et al., 1988) and also some anti-nutritional  
56 components such as, tannins, and phytic acids which can precipitate proteins (Adebooye and  
57 Singh, 2007; Khattab and Arntfield, 2009). During the cooking of the beans in hot water, the  
58 beans uptake water before starch gelatinization and protein denaturation occur. The flavor and  
59 color of the beans subsequently change with time but also with the number of the beans and  
60 the cooking media composition (Phillips et al., 1988). We hypothesis that the kinetics and all  
61 the reactions related to gelatinization of starch and denaturation of proteins would  
62 predominantly drive the cooking kinetics of cowpea seeds, given that protein and starch alone  
63 represent 60 % to 76 % of the total weight of the cowpea seeds. The water (absorption)  
64 activity can lead to substantial change of the beans' texture but it is not alone considered as  
65 cooking reaction (Borges and Peleg, 1997), although it can be kinetically activated by heat  
66 (Coffigniez et al., 2019). Thus, cowpeas beans may be considered cooked when they are  
67 gelatinized and/or denatured (Adebooye and Singh, 2007; Adebooye and Singh, 2008;  
68 Coffigniez et al., 2018; Khattab et al., 2009).

69 The evolution of the mechanical properties of a system made with similar composition may  
70 be affected by those transitions of the beans' compound states. For instance, people in their  
71 own homes use essentially the finger test as mechanical test to assess the cooking levels  
72 (Voisey, 1971). The finger test is used to evaluate how a product behaves mechanically when  
73 it is pressed between the fingers. A raw cowpea bean is shown in Fig. 1A. The state of cowpea  
74 bean after simmering at 95 °C during 60 min and 90 min is shown in Fig. 1B and 1C  
75 respectively. Fig. 1D shows how the cowpea bean that has been simmered at 95 °C during 90  
76 min (shown in Fig. 1C) looks like after being crushed between the fingers. The beans are  
77 considered well-cooked when they can easily be crushed between the fingers, and this is the  
78 way Khattab et al. (2009) have defined the cooking time (Khattab et al., 2009). Adebooye et

79 al. (2007) pressed the beans between two glass plates after every 5 min and the time when the  
80 seed yielded was considered to be the cooking time (Adebooye and Singh, 2007).

81



82

83 *Fig.1: A) Picture of a native black eye cowpea seed; and the seed after having been simmered*  
84 *for B) 60 min, C) 90 min in the water at 95 °C and D) shows the finger test applied on the*  
85 *seed of C).*

86 According to Voisey (1971), the mechanical property is the most critical criteria for assessing  
87 the texture of food, because this has the strongest influence on the acceptance of food by  
88 people and is relevant to controlling mouth feeling (Ishihara et al., 2013; Mohsenin, 1977).

89 Texture analyser is used for this purpose to have a better control of the applied forces and  
90 precision of the food's mechanical responses, to recreate the conditions of consumer  
91 interactions with the food and to correlate those results to specific sensory texture attributes.

92 In this work a mechanical compression test with a force precision of 10mN was used in order  
93 to detect the state transition from uncooked to cooked period of the cowpea seeds when they  
94 undergo cooking processes. The aim of this study was to find out how the mechanical  
95 properties constants of cowpeas seeds evolve between the beginning and the end of the  
96 reactions underlying its cooking.

97

## 99 **2. Materials and Methods**

### 100 **2.1. Materials**

101 The cowpea seeds were purchased from a local supermarket in Grenoble, France and used as  
102 such without additional treatment. A selection of the seeds based on visual appreciation  
103 criteria of the seed's surface homogeneity and cleanness was carried out and damaged seeds  
104 removed prior to the cooking method. More than 100 seeds were weighed separately using a  
105 precision Sartorius balance of 1.0 mg and the seed weight average was 0.200 g with the  
106 standard deviation of 0.023 g. The minimum and the maximum seed weight was 0.150 g and  
107 0.249 g respectively.

### 108 **2.2. Physical treatment: Soaking and heating to 95 °C**

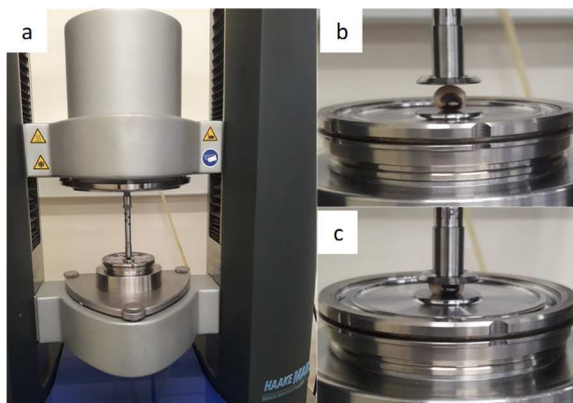
109 Four seeds were distributed in four 20 ml containers and filled with 2 g of deionized water to  
110 represent 1:10 (w/w). The containers were sealed and immediately heated to 95 °C in a water  
111 bath for 10, 30, 60, 75 and 90 min  $\pm$  3 min. The cooking time was selected based on the  
112 findings by (Coffigniez et al., 2019; Edijala, 1980; Khattab et al., 2009) who reported that at T  
113  $\geq$  95 °C, the cooking time will vary from 35 to 90 min which depends on the type of seeds  
114 and the imprecision of the finger test. Additionally, the loss of solid matter is pronounced with  
115 the heating time. Therefore only the seeds that looked intact after they had been heated were  
116 selected for the study like the ones shown earlier in Fig. 1 (A, B, C). The initial weight ( $w_i$ ) of  
117 each seed was recorded as well as the final weight ( $w_f$ ) after heating. The amount in gram of  
118 water uptake per gram of cowpea seed termed  $R_{CS}$  was determined as:

119  $R_{CS} = (w_f - w_i) / w_i$  1.

120  $R_{CS}$ , water uptake ratio calculations were carried out using four seeds per heating time in  
121 quadruplicates. The temperature in the containers reached 60 °C and 95 °C in less than 2 and  
122 5 min respectively.

123 **2.3. Compression test**

124 The test of compression was performed using the HAAKE MARS (Fig. 2a), Modular  
125 Advanced Rheometer System, Thermo Scientific instrument with a parallel geometry of 20  
126 mm of diameter (TiLL11030P20). The measurement steps were managed with the HAAKE  
127 RheoWin Job manager software 4.85.0002. The zero gap was determined and the temperature  
128 was set to 25 °C, then the geometry was raised to 10 mm. A cowpea seed was placed for each  
129 measurement between the geometry and the plate then a first step program was run to bring  
130 the geometry onto the surface of the seed (Fig. 2b). The instrument geometry stopped going  
131 down when it measured a force of 25 mN.



132  
133 *Fig.2: Picture of the experimental instrument (a) to show the onset of the compressive test (b)*  
134 *and the deformation of the seed under the compression (c)*

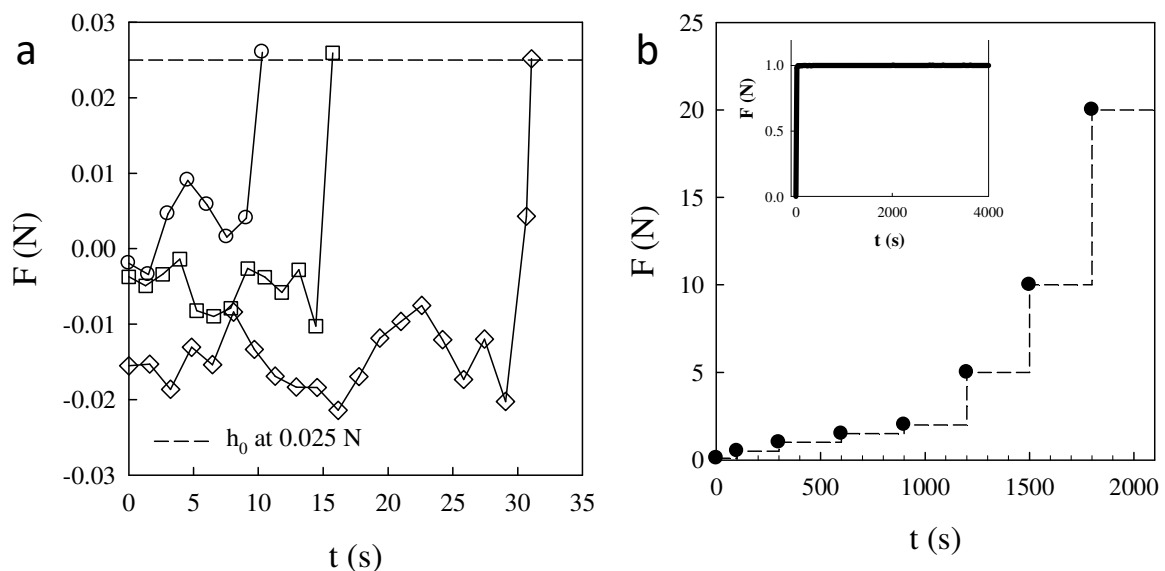
135 The force was reset to 0 at the current height, geometry position, or before the start of the  
136 compression test, the geometry position was taken as the initial height ( $h_0$ ) of the seed. The



137 height position of the geometry (Fig. 2c) during the compression ( $h_t$ ) was recorded and the  
 138 deformation ( $\varepsilon_t$ ) at time  $t$  was calculated as:

$$139 \quad \varepsilon_t = (h_0 - h_t) / h_0 \quad 2.$$

140 Three determinations of the initial height are shown in Fig. 3a. The forces detected by the  
 141 instrument fluctuated below 10 mN when the geometry ran freely, but at the moment it  
 142 touched the seed the force increased sharply and stopped at 25 mN, then the force was  
 143 immediately reset to zero, before running the compression test program. Two types of  
 144 programs were edited to study the compression of the seed. The first program (insert of Fig.  
 145 3b) was applied to investigate the deformation of the seeds over 1h at a constant load force.  
 146 The second was a multi-step loading program that consisted of a step-by-step increment of the  
 147 force during the compression (Fig.3b). This type of step-loading creep test was used by Mittal  
 148 et al. (1987) to characterize the rheological property of the apple cortex (Mittal et al., 1987).



149  
 150 *Fig.3: a) Initial height position detection test repeated 3 times (open circle, square and*  
 151 *diamond) shown as time-dependence of the force during the course of the geometry toward*  
 152 *the surface of the sample. The surface is detected when the force reaches 0.025N. b) Multiple*

153 *step force program of the compression test, the insert shows the long-time compression test*  
154 *program for  $F = 1\text{ N}$ .*

155 The compression tests were repeated four times using four seeds per heating time to give the  
156 strain plot that is the average of these four tests and its error bar is  $\pm$  the standard deviation.

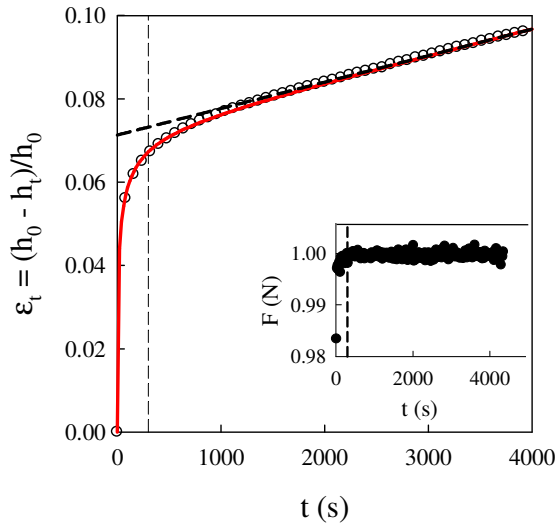
#### 157 **2.4. Data analyses**

158 Over the past three decades, some authors have investigated the uniaxial compressibility of  
159 food products in the characterization of food texture and recently Kiani Deh Kiani et al.  
160 (2009) have presumably applied the compression test at ambient temperature to determine the  
161 elasticity of red bean grains as a function of their moisture content, i.e. not in cooking  
162 conditions (Finney et al., 1964; Kiani Deh Kiani et al., 2009; Mohsenin, 1977). The time-  
163 dependence of strain with constant stress also termed creep function on the heating time is a  
164 more practical way to follow the solid-gel transition of the seeds, because the strain is time-  
165 independent for the real solid material, but time-dependent for the gel (Voisey, 1971). In the  
166 gel state and under constant stress, the seeds can behave mechanically as a solid in a short  
167 time but as a fluid in a long time. The critical time, i.e. when the behavior changes from solid-  
168 like to fluid-like, is referred to as the yield time and it has been shown that this time for  
169 polymer and colloidal gel systems is stress-dependent (Sprakel et al., 2011). Cowpea seeds  
170 are heterogeneous and the area on which the force is applied is unknown. Moreover, the  
171 contact area between the probe and the seed expands under large deformation compression  
172 forces. The factors affecting the determination of Young's modulus as well as the elastic bulk  
173 modulus when agricultural products are subjected to compressive forces are documented  
174 (Finney et al., 1964; Hamann et al., 2006; Hammerle and McClure, 1971; Mohsenin, 1977).  
175 Owing to those factors, only the force and the deformation are recorded here to account for  
176 the seed viscoelasticity when evaluating the cooking levels of the seeds. Since this implies

177 that the seeds have identical dimension to make meaningful comparison between samples of  
178 different heating times (Voisey, 1971), the analysis is based on the fact that the variation of  
179 the seed apparent area ( $S$ ) and Young's modulus ( $E$ ) depend strictly on the heating time.  
180 Consequently, the product  $E \times S$  yields a quantity termed elasticity index,  $K_e$ , in Newton unit  
181 (N), because its evolution results from  $E$ . The  $K_e$  evolution is strictly the result of the heating,  
182 which could make it possible to distinguish the uncooked and cooked cowpea seeds. The  
183 Poisson's ratio is odd in large deformations of food products (Kiani Deh Kiani et al., 2009;  
184 Voisey, 1971).

185 The compression test at 1 N of a cowpea seed soaked in demineralized water and heated for  
186 10 min is presented in Fig. 4. The height of the seed decreased sharply at first exponentially  
187 then asymptotically over the critical time. The insert of the Fig. 4 shows the force profile with  
188 a dash line to represent the time it takes for the instrument to load the force. The time  
189 evolution of the height during the loading stage is the result of the coupling between the  
190 loading activity and the viscoelastic response of the sample. This stage could be affected by  
191 the loading speed capacity of the instrument, therefore one should keep in mind that it is not  
192 only the seed response but it could also be an experimental imperfection. However, this  
193 loading phase is fundamental for understanding the behavior of the sample afterward. For a  
194 perfectly elastic material for instance, the loading stage would not be critical, because the  
195 elastic constant is time-independent. However, viscoelastic materials above yield stress have  
196 demonstrated time-dependent mechanical behavior (Kiani Deh Kiani et al., 2009; Mittal et al.,  
197 1987; Nussinovitch et al., 1990). Given that the current sample subsequently exhibited flow  
198 behavior, it cannot be excluded that the force-loading rate influences the sample's  
199 microstructure and consequently the flow property. The experimental condition could have  
200 been difficult, if the samples have experienced severe aging in the time interval of the

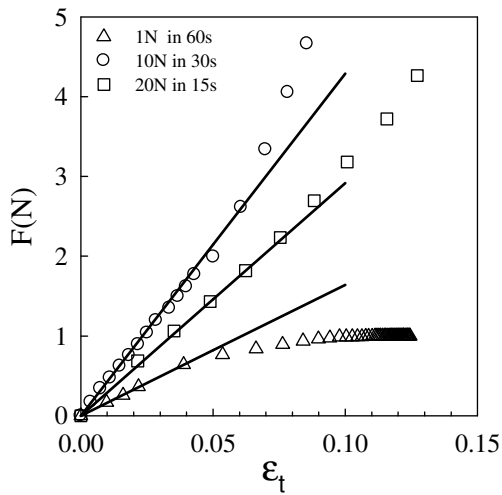
201 measurement because aging could affect the mechanical behavior (Kouemene et al., 2013;  
 202 Landrum et al., 2016).



203  
 204 *Fig. 4: Time-dependence of deformation  $\varepsilon_t$  of a cowpea seed after heating the seed at 95 °C*  
 205 *for 10 min as a result of loading 1 N force (insert). The vertical dash line is the time where*  
 206 *the force is reached. The continuous line through the data is the fit to equation (1) with  $\omega$  the*  
 207 *slope of the dash line like the asymptote of the creep evolution ( $\omega t^\beta + \varepsilon$ ), and  $\varepsilon$  is where the*  
 208 *asymptote crosses the time 0 axis. The fit parameters are:  $t_c = 23$  s,  $\alpha = 0.35$ ,  $\beta = 1$ ,  $\varepsilon = 7.13$*   
 209 *%,  $\omega = 6.35 \times 10^{-6} \text{ s}^{-1}$ .*

210 The time necessary for a material to undergo phenomena of disorganization and to start to  
 211 flow depends on several factors that excite the curiosity of many authors (Coussot, 2014;  
 212 Sprakel et al., 2011). The deformation here showed a good coefficient of linear correlation  
 213 with the forces during the force-loading period, but its consistency was highly time-dependent  
 214 (Fig. 5). The linear response domain of the cowpea seed seemed to increase with increasing  
 215 loading rate. Elsewhere, Kiani Deh Kiani et al (2009) found that the Young's modulus of red  
 216 bean seed increased with increasing loading rate (Kiani Deh Kiani et al., 2009). With the  
 217 exception of the imperfection experimental instrument (Voisey, 1971) these observations are

218 the results of time-dependent disorders or phenomena of changing of state which occurs in  
219 food materials as soon as they have been strained (Coussot, 2014).



220

221 *Fig. 5: Deformation dependence of loading forces on seeds after heating at 95 °C for 10 min.*  
222 *The forces and the times it takes to load the forces are indicated in the legend. The seeds*  
223 *respond elastically in the beginning of the loading force. The higher the force that is loading,*  
224 *the faster the loading process and the higher the elastic deformation domain. This*  
225 *observation reflects the impact of the loading rate on the compliance of the samples.*

226 These disorder phenomena convert part of the working energy to entropy energy, the  
227 conversion time depends on the kinetic of the reactions mechanisms (Landrum et al.,  
228 2016).The material exhibits apparent elastic property if the increase of the load rate  
229 compensates the loss of energy. If the loading is done faster than the relaxation time of the  
230 material, then the material tends to behave like a perfect solid. Interestingly, the samples in  
231 this study exhibit a constant flow rate defined by the slope of the asymptote in Fig. 4. A  
232 similar creep curve was found with gellan gel (Nussinovitch et al., 1990). This means that, if a  
233 linear relationship between the applied force and the flow rate is verified, then a quantity in  
234 N.s unit reflecting the viscosity of the material could be determined. This quantity is referred  
235 to as the viscosity index,  $K_v$ . The applied force was plotted against the sample flow rate after

236 performing the compression test at different constant forces. However, the result was noisy  
 237 which was likely due to the fact that a new seed prepared in the same condition was loaded  
 238 onto the rheometer when the applied force was changed. The three plots of the Fig. 5 clearly  
 239 demonstrate the impact of the physical characteristic of the seeds on the reproducibility of the  
 240 data, given that the elastic index,  $K_e$ , corresponding to the three seeds of identical preparation  
 241 yielded 16.42 N, 42.9 N, and 29.17 N with an average of  $29.5 \pm 13$  N. We believe that the  
 242 native composition and the dimensions of the seeds could be the main causes of the noise as  
 243 these affect the axial deformation. Indeed, the error on the deformation,  $d\varepsilon$ , can be expressed  
 244 as the sum of errors due to: -i) the applied forces (F),  $d\varepsilon_F$ , as instrumental imperfection; ii)  
 245 elastic modulus (E),  $d\varepsilon_E$ , as the variation of the seed composition; and (iii) the area (S) over  
 246 which the applied forces are distributed,  $d\varepsilon_S$  as the seed dimensions. If the elastic modulus of  
 247 the seeds is assumed identical and the errors on the applied force are neglected then the error  
 248 on the deformation is geometrical as

$$249 \quad d\varepsilon = d\varepsilon_s = \left( \frac{dS}{S} \right) \cdot \varepsilon \quad 3.$$

250 Although the precise values of the elastic modulus is somewhat uncertain, the creep behavior  
 251 for mostly all the samples is quite clear. Given that mostly all the samples tested in this study  
 252 displayed the same creep behavior, we tried the model of Eq.(4) to sort out some  
 253 characteristic parameters for the discussion on the mechanical properties of these complex  
 254 systems. The strain was calculated and then the plot was fitted to Eq.(4) to obtain the values  
 255 of the fit parameters.

$$256 \quad \varepsilon_t = (\varepsilon_0 - \varepsilon) \cdot e^{-N_t} + \omega \cdot t^\beta + \varepsilon \quad 4.$$

$$257 \quad \text{with } N_t = (t/t_c)^\alpha \quad 5.$$

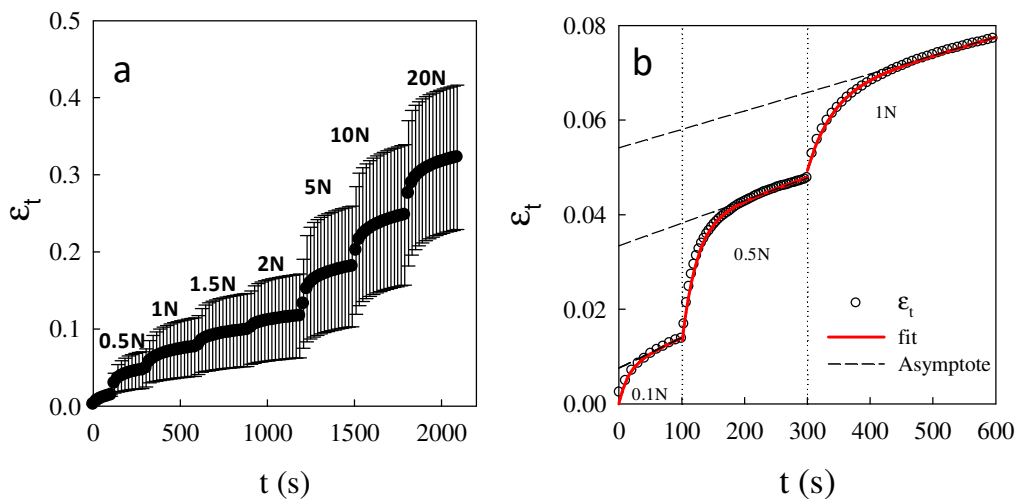
258 The fit function, Eq. (4), is a combination of the first period where the response of the  
259 material to the loading force is elastic-like, and the second period is the flow (creeping) at  
260 constant force. The  $t_c$  in the  $N_t$ , Eq. (5), gives the characteristic compliance time during the  
261 loading phase. The flow of the material takes place in this case following disorder events  
262 occurring during compliance. The  $\alpha$  in  $N_t$  is time structural factor of disordering events that  
263 occur in the material. The events can occur from time to time instead of being continuous as  
264 the internal dynamics are very weak to consider that they occur freely. The parameter  $\varepsilon_0$   
265 defines the initial condition of the deformation. For the flow part of the function,  $\omega$  and  $\varepsilon$  are  
266 the constants of the regression function when applicable and they mean the flow rate and the  
267 axial deformation of the seed respectively. The constant  $\varepsilon$  is represented by the intersection  
268 between the y-axis and the function  $\omega t^\beta + \varepsilon$  at  $t_0$ , so  $\varepsilon$  is somehow the onset of the elastic  
269 response to the applied constant load. The adjusting parameter  $\beta$  can take 1 for all the  
270 analysed measurement, but if necessary, a value between 0.95 and 1 was tested to have the  
271 best adequacy with the measurement. Unless otherwise indicated, the value of  $\beta$  is 1. For the  
272 current samples, the Fig. 4 shows the adjustment and the regression function of the flow part.  
273 Both functions are plotted in solid and dashed lines respectively. The values of the adjustment  
274 parameters are also indicated in the legend. The flow rate,  $\omega$ , of the seed was found to be  
275  $6.35 \times 10^{-6} \text{ s}^{-1}$ . The current seed felt like hard chewing gum when pressed between the fingers  
276 implying that the seed in this state is not yet soft to be eaten (Khattab et al., 2009).

### 277 **3. Results and discussion**

#### 278 **3.1. Deformation under incremental compressive forces**

279 The average of the strain from the measurement of the 4 seeds after 10 min in water at 95 °C  
280 is shown in Fig. 6a. The standard deviation per the average strain yields a value  $\delta$  that  
281 fluctuate between 10 % and 50 %. The median of  $\delta$  values yields 30 %, i.e. 50 % of  $\delta$  values

282 are below 30 % and 50 % of  $\delta$  values are above 30 %. This fluctuation was also observed for  
 283 all the other quantities that were determined (i.e. viscosity indices, elasticity indices, flow  
 284 rate, etc.). Therefore, unless otherwise indicated, considering a quantity  $\Psi$  of the mechanical  
 285 tests, the standard deviation of the average can be taken as 30 % of the average in this present  
 286 study. For the sake of clarity, only the averages of the strain-time plots are displayed in Fig.  
 287 6b. The plots were analysed using the fit function (full line), the dash lines show the linear  
 288 regression function of the flow part of the samples and the points where they meet the time 0  
 289 axis. The time delay between the forces (dotted lines) was decided according to the previous  
 290 tests on the samples of the same series and the compression test program was adjusted to fit  
 291 with the samples behavior.



292  
 293 *Fig.6: a) Time-dependence of deformation  $\epsilon_t$  of a cowpea seed after heating the seed at 95°C*  
 294 *for 10 min as a result of loading multiple forces. The error bars are the standard deviation*  
 295 *calculated on the average of 4 seeds. b) is the zoom in to the 0.1 N, 0.5 N and 1 N to show the*  
 296 *fit to equation (1) and the crossing point of the asymptote with the time 0 axis. For the error*  
 297 *bars of Fig. 6b see Fig. 6a or apply 30 %  $\times \epsilon_t$  to get the standard deviation.*

298 The cowpea seeds behave instantly as an elastic material when the applied force was  
 299 increased before going under constant flow rate a few seconds after the forces have reached



300 the plateau. It is noteworthy mentioning that the time delay between the forces was not  
301 changed (increased for instance) to see the impact of this on the behavior of the samples. This  
302 will be tested in another study.

303 The compression test was carried out in an unconfined state, so the seeds expanded  
304 transversally by the flow behavior but not as an incompressible fluid. There are a number of  
305 factors that can make the compression to stop. These are: i) when locally the concentration  
306 increases and the compressibility of the seeds decreases as the volume decreases towards the  
307 total volume of the uncompressed elementary constituents. The deformation of the seeds will  
308 be stopped by the exclusion effect of the elementary constituents, i.e. limit of the samples  
309 compressibility; and ii) when the geometry reaches the zero gap. The measurements did not  
310 show any remarkable tendency towards stability which means that the maximum degree of  
311 compaction was not attained for all the mechanical tests. The time between the application of  
312 load and the moment when the sample yields which is the yield or critical time, generally  
313 depends on the applied force because yielding mechanism are an activated energy process.  
314 The critical time and stress relationships vary from one system to another. It depends on the  
315 competition and the cooperative or synergistic effects of the many yielding events that can  
316 take place in the seed at any instant. The thermal motion of small molecules and reptation of  
317 biopolymers (De Gennes, 1976), the balance between the dynamic of physical bonds rupture  
318 and reconstruction (Sprakel et al., 2011) are some of the fundamental yielding events of  
319 which the kinetics determine the critical time of the creep behavior of the samples.

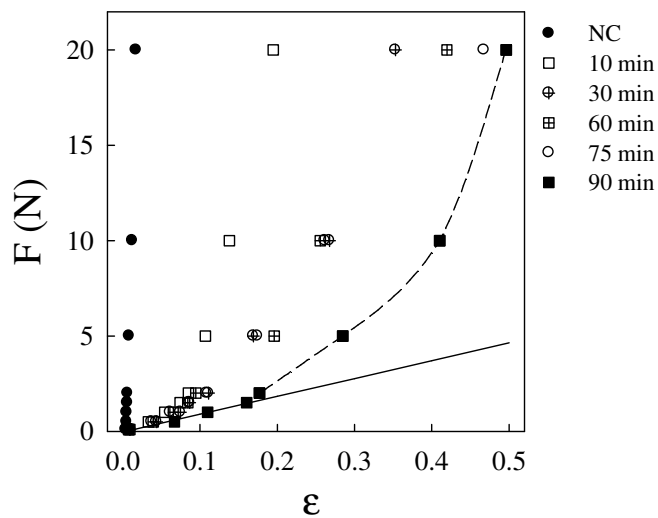
320 The critical time,  $t_c$ , and  $\alpha$  of the fit function are related to the time behavior of the sample  
321 under yielding. The values of  $\alpha$  fluctuate between 0.5 and 1 when the values of  $t_c$  fluctuate  
322 between 14 s and 70 s with the change of the applied forces. This means that a clear  
323 correlation between the parameter  $\alpha$  or  $t_c$  with the applied forces was not observed in the  
324 present study. Thus, it was not possible to correlate afterward the critical time with the heating

325 time of the seeds and this implies the complexity of characterizing the yield time of  
326 heterogeneous condensed materials under mechanical stress. For instance, it is demonstrated  
327 that the relaxation time of polymer and colloidal systems exhibit an exponential decay  
328 dependence on the applied stress (Sprakel et al., 2011), but for a mixture of polymer and  
329 colloidal system or for heterogeneous systems in general this relationship is not  
330 fundamentally confirmed. Cowpea seed systems consist of a tightly wrapped packs of starch  
331 granule cells in a protein matrix around which there are hydrocolloids and low presence of fat  
332 (Coffigniez et al., 2019; Swanson et al., 1985). The compression test of this system has shown  
333 yielding despite of the applied forces (between 100 mN to 20 N) demonstrating the weakness  
334 of the energy needed to activate the yielding mechanisms. The absorption of water by the  
335 seeds which causes the microstructure to swell and the intercellular spaces to increase is  
336 pronounced by heat, capillary effects, and by the pectin and protein based substances through  
337 the migration process in order to balance the osmotic pressure (Coffigniez et al., 2019).  
338 Although the appearance of the whole seed seemed to be preserved, some of the walls of the  
339 interfacial cells could have been damaged and water may continue to diffuse into the whole  
340 seed until the osmotic pressure is balanced even at room temperature. The dynamic of the  
341 system to reach equilibrium would have been enhanced by a local increase of temperature due  
342 to the effects of stress. The lubrication of the interstitial spaces between the seeds cells and  
343 their large clusters due to the presence of lipid substances in the intercellular spaces would be  
344 also enhanced by the locally induced increase of temperature by stress. It is noteworthy to  
345 mention that after 10 min in water at 95 °C the seeds have taken on average about  $0.4 \pm 0.3$  g  
346 of water per gram of seeds.

### 347 **3.2. Compressive force and deformation relationships upon heating time**

348 It is shown earlier (in Fig. 5) that the instantaneous responses of the samples are elastic before  
349 the elastic response of the sample give way to flow response when the imposed forces are

350 completely loaded. Therefore, the intersection between the (asymptotic) flow function and  
 351 time 0 axis is taken here as the instantaneous elastic deformation,  $\varepsilon$ , and assigned to the  
 352 applied force. Fig.7 shows the results for different heating times at 95 °C and time 0 for the  
 353 uncooked (native cowpea) beans , which is denoted as NC.

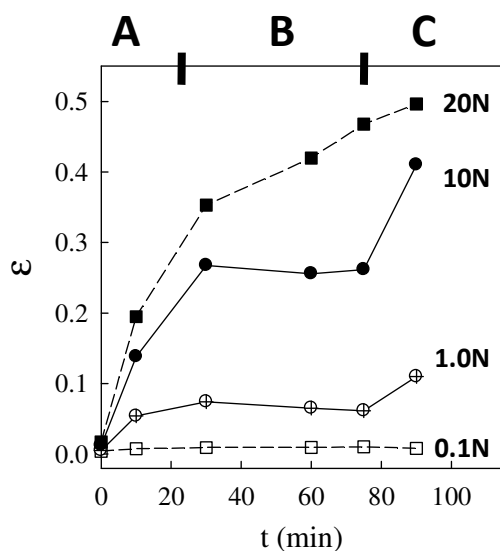


354  
 355 *Fig.7: Applied forces as function of the deformation  $\varepsilon$  for the native cowpea seed (NC) and*  
 356 *the different times of heating the seeds at 95 °C. The full line through the data shows the*  
 357 *elastic domain for the seeds after heating at 95 °C for 10 min and the slope reflects the elastic*  
 358 *constant in N unit. The dash line is a guide for eyes. Apply 30 %  $\times \varepsilon$  for horizontal standard*  
 359 *deviation.*

360 The force as the functions of deformation increases quite linearly as shown by the full line  
 361 through the data of 90 min and deviates from linearity with higher slope. The compression  
 362 tests of alginate gels have shown practically similar trend, which the authors have described  
 363 by a concave upward function using a power-law model, where the pre-factor was referred to  
 364 as the gel stiffness and the power as the degree of concavity that reflects the deviation from  
 365 linearity. When the power equal 1, then the power-law model reduces to Hooke's law and the  
 366 pre-factor coincides with the modulus of elasticity (Mancini et al., 1999). Given that the slope

367 is characteristic of the seeds elasticity, the increase of this means strengthening of the seed.  
 368 However, under unconfined compressive force, this trend may reflect the compaction effects  
 369 requiring additional force to strain the sample rather than strain hardening effects (Mancini et  
 370 al., 1999). Furthermore, the resistance to stretch the seed coat could explain the rising of the  
 371 force-deformation function. At higher compressive forces, the deformation amplitude  
 372 decreases from the native seed with increasing heating time. However, the way it decreases  
 373 seems to depend on the applied forces.

374 Fig. 8 shows for each applied force the deformation values as a function of the heating times.  
 375 The results in this figure mimic taking one seed after the other for each heating time and  
 376 crushing it between fingers or teeth to check whether the seeds are cooked or not. The scale of  
 377 A to C shown on the top axis of Fig. 8 represents how the seed felt between the fingers or  
 378 teeth where: A = Uncooked or not edible; B = cooked a little but firm on teeth, i.e. "al-dente";  
 379 C = cooked or well-done, i.e. melt in mouth.



380  
 381 *Fig.8: The deformation of the Fig. 7 is plotted as a function of the heating time at 95 °C when*  
 382 *the forces indicated in the figure are applied. The finger test A, B, and C on the top axis*  
 383 *represent how the cowpea seed was perceived by different people where A = Uncooked or not*

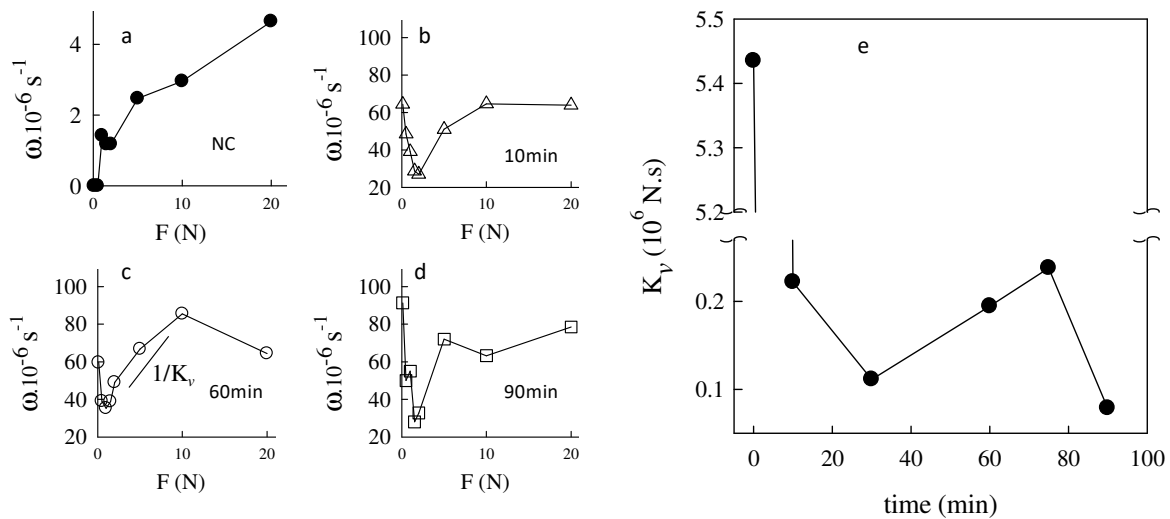
384 *edible; B= cooked a little like firm on teeth, i.e. "al-dente"; C= cooked or well done. Apply 30*  
385 *% × ε for vertical standard deviation and ± 3 min for horizontal (time) error bars.*

386 At a weak or strong applied forces, i.e. 0.1 N or 20 N, the deformation of the seed evolves  
387 without a significant discriminative signature between the cooking levels. For the curve of 20  
388 N, the change of the slope is weak between A and B and is absent between B and C. For the  
389 curve of 0.1 N, the deformations are too weak to provide relevant information on the periods  
390 of the cooking reactions. Therefore, the sort by cooking-level of the seed is weakly precise  
391 with both extreme forces. However, for intermediate compressive forces, the test shows a  
392 remarkable transitional phase that is characterized by a plateau between level A and C. The  
393 controlling compressive forces show a clear-cut between uncooked and cooked seeds as long  
394 as the compression test is done with moderate applied forces.

### 395 **3.3. Compressive deformation rate and the seed viscosity index**

396 The deformation rates ( $\omega$ ) of the seeds are plotted as function of the applied forces to the  
397 different heating times. Four graphs are displayed in Fig. 9 to illustrate the force-dependence  
398 of  $\omega$ . These graphs are; the raw seed (NC, Fig. 9a) and the seed after heating time of 10 min  
399 (Fig. 9b), 60 min (Fig. 9c) and 90 min (Fig. 9d) at 95 °C. The graph of the native seed shows  
400 no deformation rate for the lowest compressive forces where as  $\omega$  starts increasing from  
401 roughly 1 N (Fig. 9a). The rise of  $\omega$  from a stress threshold could characterize the heated  
402 seeds too, although it is not seen in the figures 9 b, c, and d, which is mainly attributed to the  
403 fact that the yield stress is lower than the forces applied in this case. Indeed, the overall seeds  
404 exhibit time-dependent yielding behavior which energy barrier stem from the physical bonds  
405 that provide to the seeds the resistance against flow under their own weight. The fact that  $\omega$   
406 decreases first for the seeds of Fig. 9 b, c, d suggests that free liquid exuded out of the seeds  
407 cell interstices. Such expulsion leads to compaction as a result of which  $\omega$  decreases to a

408 minimum that reflects presumably the transition between the liquid removal and a jamming  
 409 flow regime. In the jamming regime,  $\omega$  increases from the minimum around  $30 \pm 10 \times 10^{-6} \text{ s}^{-1}$   
 410 to a maximum around  $75 \pm 10 \times 10^{-6} \text{ s}^{-1}$  with increasing applied forces (N) for the heated seeds  
 411 but the maximum for the native seeds was not reached. The  $\omega$  of the native seeds is 10 to 20  
 412 times lower than that of the heated seeds. The deformation rate is assumed to evolve with the  
 413 applied forces linearly in the jamming flow regime. This assumption made it possible for the  
 414 viscosity index,  $K_v$ , to be calculated.



415  
 416 *Fig.9: Force-dependence of deformation,  $\omega$ , of native cowpea (a), heating times in the figures*  
 417 *(b,c,d) at 95 °C reflect the evolution of the seeds viscosity ( $K_v$  in N.s unit) as a function of the*  
 418 *heating time, time 0 is NC, (e).  $K_v$  is given by considering  $\omega$  as linear with F in the increasing*  
 419 *(jamming) domain. Note that the break on the y-axis shows the amplitude of the loss of the  $K_v$*   
 420 *of the cowpea once it starts to cook and the time domain where  $K_v$  increases and this shows*  
 421 *the transitioning between uncooked and cooked state. Apply 30 %  $\times$  ( $K_v$ ,  $\omega$ ) for vertical*  
 422 *standard deviation and  $\pm 3$  min for horizontal (time) error bars.*

423 The compressive viscosity index,  $K_v$ , decreases catastrophically between the native seeds and  
 424 the seeds after 10 min of heating. The decrease continues weakly between 10 min and 30 min

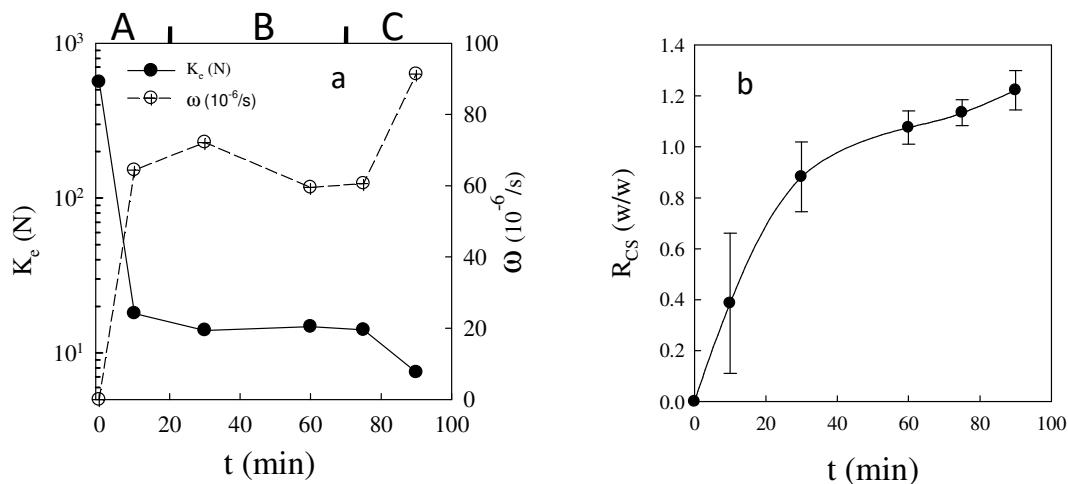
425 heating time and rises between 30 min and 80 min, where presumably: (i) gelatinization of  
426 starch (Adebooye and Singh, 2008; Biliaderis et al., 1980; Kong et al., 1999); (ii) denaturation  
427 with aggregation of protein (Tolkach and Kulozik, 2007); and (iii) hydration of carbohydrate  
428 like pectin, significantly take place (Coffigniez et al., 2019). At the end of these processes,  
429 after 80 min, the  $K_v$  decreases continuously because of additional absorption of water (Fig. 9e)  
430 until the seeds burst.

### 431 **3.4. Seeds stiffness and flow rate as function of the heating time**

432 The relation between  $\varepsilon$  and the applied forces were interrogated to derive the elastic  
433 coefficient according to Hooke's law termed elasticity index,  $K_e$  in N unit. The  $K_e$  is the  
434 constant of proportionality between the applied forces and the deformation in the elastic like  
435 domain, i.e. before the deformation deviates from linearity. The  $K_e$  values are plotted as  
436 function of the heating time (result of native seeds is represented by time zero) on the left axis  
437 of Fig. 10a in a log-lin scale. The deformation rates,  $\omega$ , at 0.1 N are plotted on the same figure  
438 (Fig. 10a) as function of the heating time using the right axis. The cooking level A, B, C are  
439 presented on the top axis of the heating time. The Fig.10b shows the evolution of the water  
440 uptake by the seeds.

441 During the first 10 min, the elasticity index,  $K_e$ , of the seeds decreases steeply from 560 N to  
442 19 N, a loss of 97 % of their initial stiffness owing to the flow of water into the seeds  
443 macrostructure. The water uptake by the seeds during the first 10 min was on average 38 % of  
444 the seeds weight. As a result of this absorption of water by the seed, the flow rate of the seeds  
445 significantly increased. When the heating time was increased from 10 min to 30 min, the  
446 seeds lost 36 % of their stiffness and the seeds flow rate  $\omega$  increased weakly. However the  
447 amount of water uptake by the seeds in this second period increased by 50 % with almost a  
448 constant rate. The decrease of the stiffness during the heating period from 10 min to 30 min is

449 not a result of the absorption of water alone but also a consequence of a collection of  
 450 mechanisms with opposing effects that prevent both the catastrophic decrease of the stiffness  
 451 and thickness of the seeds. Thus, we suggest that the gelatinization of starch and denaturation  
 452 of protein processes in this heating period strengthen the seeds. These processes define the  
 453 onset of the cooking rather than the water absorption alone. Therefore, it could be  
 454 hypothesised that the cooking of the seeds starts between 10 min and 30 min at 95 °C.



455  
 456 *Fig.10: (a) Evolution of the elasticity constant,  $K_e$  on the left axis, and the deformation rate*  
 457 *( $\omega$ ) on the right axis for 0.1 N as a function of the heating time of the seed at 95 °C. Apply 30*  
 458 *%  $\times$  ( $K_e$ ,  $\omega$ ) for vertical standard deviation and  $\pm 3$  min for horizontal (time) error bars. (b)*  
 459 *Water uptake in w/w of cowpea seeds as function of the heating time at 95 °C. Error bars are*  
 460  *$\pm$  the standard deviation computed on 4 seeds for each heating time.*

461 When the heating time was between 30 min and 80 min, the  $K_e$  remained practically constant  
 462 at 14 N, although the absorption of water by the seeds was shown to slightly increase. We  
 463 could say that the cooking reactions contribute to the stability of the  $K_e$  until the end of the  
 464 reactions somewhere between 75 min and 90 min. Beyond 75 min the stiffness and the  
 465 thickness of the seeds reduces catastrophically. Heating time longer than 90 min destroyed the  
 466 seeds and their internal contents were expelled in the cooking media (Edijala, 1980).



#### 467 **4. Conclusion**

468 Cowpea is rich in protein (20 % - 26 % w/w) and starch (40 % - 70% w/w), it contains also  
469 vitamin, fat and hydrocolloids but in weak proportion. Cowpea seeds are multiple varieties of  
470 species of which the size, weight, seeds coat texture and composition are the specific  
471 attributes. Seeds without visual defects were selected to investigate the seeds cooking time  
472 using the mechanical compression test given that the mechanical properties of food are  
473 correlated with the physical and chemical changes of the food. However: i) how the seeds will  
474 behave when they are subjected to mechanical test; ii) how their mechanical properties are  
475 correlated with the seeds transformations; and iii) whether this correlation will allow  
476 independently food engineers to visualize the transitioning of the seeds to the cooked state  
477 cannot be predicted. The seeds are cooked when the physical and chemical reactions  
478 underlying the seeds cooking are done. Therefore, we think that the activation of both protein  
479 denaturation and starch gelatinization reactions are the starting point of the seed cooking,  
480 although before these reactions happen the seeds uptake water during cooking at 95°C. We  
481 found that cooking of the seeds starts between 10 min and 30 min because the seeds stiffness  
482 (elasticity index) and thickness (viscosity index) decrease weakly during this period of time.  
483 Before this period both mechanical constants decreased strongly, for instance a loss of 97 %  
484 of the elasticity index was observed during the first 10 min of heating of cowpea seeds. The  
485 time the seeds are cooked was found to be between 75 min and 90 min, because in this period  
486 it was observed that both mechanical constants decrease sharply. Furthermore just before, i.e.  
487 between 30 min and 75 min, the stiffness was practically constant, and the thickness was  
488 increasing or the flow rate was decreasing. To get the stiffness (elasticity index) and the  
489 thickness (viscosity index), a stretched exponential plus a linear asymptotic time function was  
490 used to fit the creep behavior of the sample where the strain ( $\epsilon$ ) and the flow rate ( $\omega$ ) were the  
491 fit functions parameters. These fit parameters correlate respectively with the applied forces

492 within the linear regime. Viscoelasticity indices correlate with the cooking reaction  
493 transitioning.

494 This work allow to investigate the influence of the cooking medium (salt, pH, sugar, etc.) and  
495 other physical seed treatment (from harvest to cooking) on the cooking time and the way the  
496 legumes behave mechanically when the undergo cooking reactions in order to achieve  
497 commercially acceptable new foods textures with reduction of the cooking energy.

## 498 **5. Acknowledgment**

499 The authors declare no conflicts of interest. This work was financially supported by the  
500 educational ministry of TOGO. The Laboratoire Rhéologie et Procédés (LRP) is part of the  
501 LabEx Tec 21 (Investissements d'Avenir - grant agreement n°ANR-11-LABX-0030) and of  
502 the PolyNat Carnot Institut Investissements d'Avenir - grant agreement n°ANR-11-CARN-  
503 030-01).

## 504 **6. References**

- 505 Adebooye, O.C., Singh, V., 2007. Effect Of Cooking On The Profile Of Phenolics, Tannins,  
506 Phytate, Amino Acid, Fatty Acid And Mineral Nutrients Of Whole-Grain And  
507 Decorticated Vegetable Cowpea (*Vigna Uguiculata L. Walp*). *Journal of food*  
508 *Quality*, 30, 1101-1120.
- 509 Adebooye, O.C., Singh, V., 2008. Physico-chemical properties of flours and starches of two  
510 cowpea varieties (*Vigna Unguiculata (L.) Walp*). *Innovative Food Science and*  
511 *Emerging Technologies*, 9, 92-100.
- 512 Biliaderis, C.G., Maurice, T.J., Vose, J.R., 1980. Starch gelatinization phenomena studied by  
513 differential scanning calorimetry. *Journal of Food Science*, 45, 1669-1674.

514 Borges, A., Peleg, M., 1997. Effect of Water Activity on the Mechanical Properties of  
515 Selected Legumes and Nuts. *Journal of Science Food and Agriculture*, 75, 463-471.

516 Coffigniez, F., Briffaz, A., Mestres, C., Akissoé, L., Bohuon, P., El Maâtaoui, M., 2019.  
517 Impact of soaking process on the microstructure of cowpea seeds in relation to solid  
518 losses and water absorption. *Food Research International*, 119, 268-275.

519 Coffigniez, F., Briffaz, A., Mestres, C., Alter, P., Durand, N., Bohuon, P., 2018. Multi-  
520 response modeling of reaction-diffusion to explain alpha-galactoside behavior during  
521 the soaking-cooking process in cowpea. *Food Chemistry*, 242, 279-287.

522 Coussot, P., 2014. Yield stress fluid flows: A review of experimental data. *Journal of Non-  
523 Newtonian Fluid Mechanics*, 211, 31-49.

524 De Gennes, P.G., 1976. Dynamics of Entangled Polymer Solution. *Macromolecules*, 9, 594-  
525 598.

526 Edijala, J.K., 1980. Effects of processing on the thiamin, riboflavin and protein contents of  
527 cowpeas (*Vigna unguiculata (L) Walp*). I. Soaking, cooking and wet milling processes  
528 *Journal of Food Technology*, 15, 435-443.

529 Finney, E.E., Hall, C.W., Thompson, N.R., 1964. Influence Of Variety And Time Upon The  
530 Resistance Of Potatoes To Mechanical Damage. *American Potato Journal*, 41, 170-  
531 186.

532 Hamann, D.D., Zhang, J., Daubert, C.R., Foegeding, E.A., Diehl, K.C., 2006. Analysis Of  
533 Compression, Tension, And, Torsion For Testing Food gel Fracture Properties.  
534 *Journal of texture Studies*, 37, 620-639.

535 Hammerle, J.R., McClure, W.F., 1971. The Determination Of Poisson's Ratio By  
536 Compression Tests Of Cylindrical Specimens. *Journal of Texture Studies*, 2, 31-49.

537 Ishihara, S., Nakao, S., Nakauma, M., Funami, T., Hori, K., Ono, T., Kohyama, K., Nishinari,  
538 K., 2013. Compression Test Of Food Gels On Artificial Tongue And Its Comparison  
539 With Human Test. *Journal of Texture Studies*, 44, 104-114.

540 Khattab, R.Y., Arntfield, S.D., 2009. Nutritional quality of legume seeds as affected by some  
541 physical treatments 2. Antinutritional factors. *Food Science and Technology*, 42,  
542 1113-1118.

543 Khattab, R.Y., Arntfield, S.D., Nyachoti, C.M., 2009. Nutritional quality of legume seeds as  
544 affected by some physical treatments, Part 1: Protein quality evaluation. *Food Science  
545 and Technology*, 42, 1107-1112.

546 Kiani Deh Kiani, M., Maghsoudi, H., Minaei, S., 2009. Determination of Poisson's ratio and  
547 Young's modulus of red bean grains. *Journal of Food Process Engineering*, 34, 1573-  
548 1583.

549 Kong, C.S., Ogawa, H., Iso, N., 1999. Compression Properties Of Fish-Meat Gel As Affected  
550 By Gelatinization Of Added Starch. *Journal of Food Science*, 64, 283-286.

551 Kouemene, T.V.D.P., Bitjoka, L., Ntamack, G.E., Tonye, E., 2013. Evaluation of  
552 Temperature and Mechanical Properties of Beans during Cooking Process.  
553 *International Journal of Science and Technology*, 3, 118-124.

554 Landrum, B.J., Russel, W.B., Zia, R.N., 2016. Delayed yield in colloidal gels: Creep, flow,  
555 and re-entrant solid regimes. *Journal of Rheology*, 60, 783-807.

556 Mancini, M., Moresi, M., Rancini, R., 1999. Uniaxial Compression And Stress Relaxation  
557 Tests On Alginate Gels. *Journal of Texture Studies*, 30, 639-657.

558 Mittal, J.P., Mohsenin, N.N., Sharma, M.G., 1987. Rheological Characterization Of Apple  
559 Cortex. *Journal of texture Studies*, 18, 65-93.

560 Mohsenin, N.N., 1977. Characterization And Failure In Solid Foods With Particular  
561 Reference To Fruits And Vegetables. *Journal of Texture Studies*, 8, 169-193.

562 Nussinovitch, A., Ak, M.M., Normand, M.D., Peleg, M., 1990. Characterization Of Gellan  
563 Gels By Uniaxial Compression, Stress Relaxation and Creep. *Journal of Texture*  
564 *Studies*, 21, 37-49.

565 Phillips, R.D., Chinnan, M.S., Branch, A.L., Miller, J., McWatters, K.H., 1988. Effects of  
566 Pretreatment on Functional and Nutritional Properties of Cowpea Meal. *Journal of*  
567 *Food Science*, 53, 805-809.

568 Sprakel, J., Lindström, S.B., Kodger, T.E., Weitz, D.A., 2011. Stress Enhancement in the  
569 Delayed Yielding of Colloidal Gels. *Physical Review Letters*, 106.

570 Swanson, B.G., Hughes, J.S., Rasmussen, H.P., 1985. Seed Microstructure: Review Of Water  
571 Imbibition In Legumes. *Food Microstructure*, 4, 115-124.

572 Tolkach, A., Kulozik, U., 2007. Reaction kinetic pathway of reversible and irreversible  
573 thermal denaturation of b-lactoglobulin. *Lait*, 87, 301-315.

574 Voisey, P.W., 1971. Modernization Of Texture Instrumentation. *Journal of Texture Studies*, 2,  
575 129-195.

576

577

## Figures



**Fig. 1**

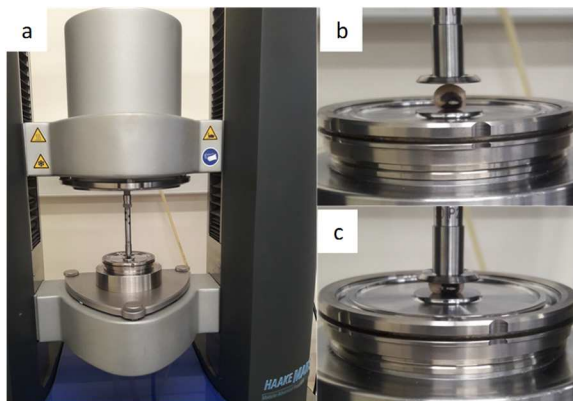


**Fig. 2**

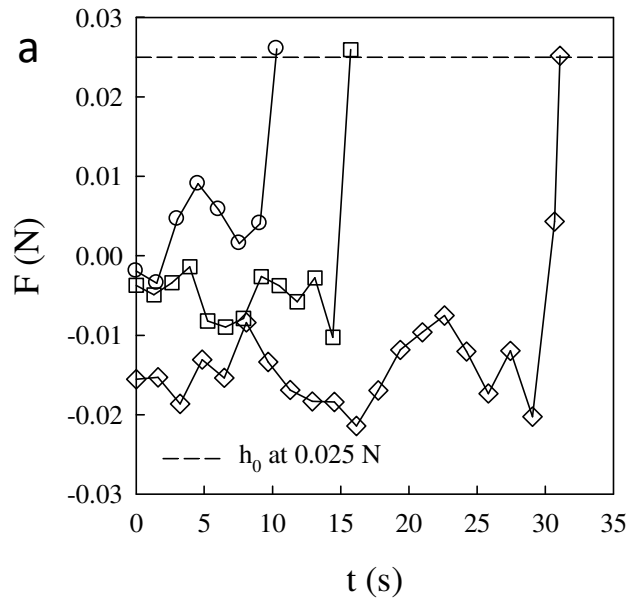


**Fig. 3a**

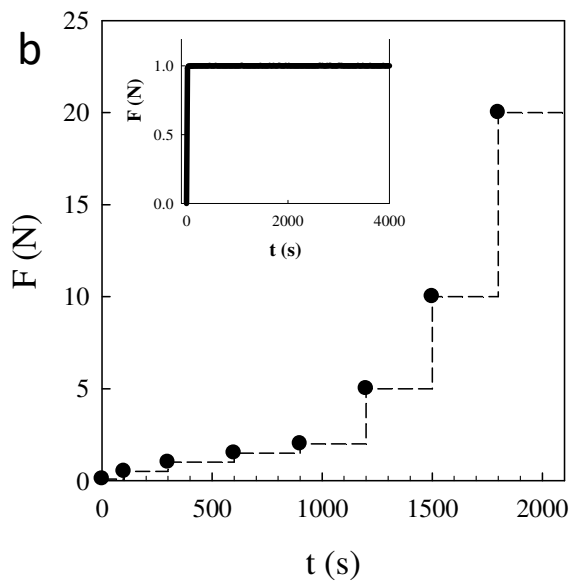


**Fig. 3b**

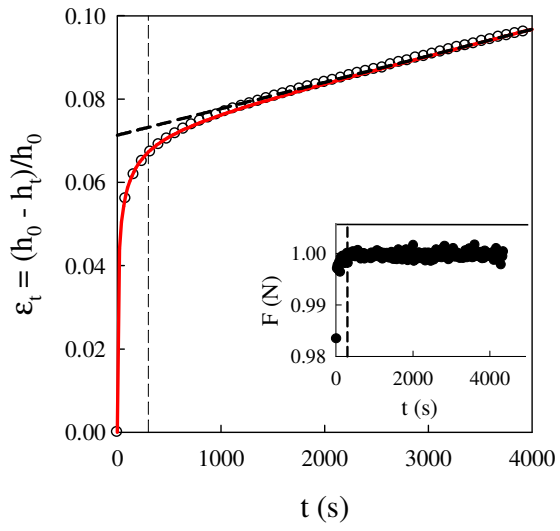


**Fig. 4**

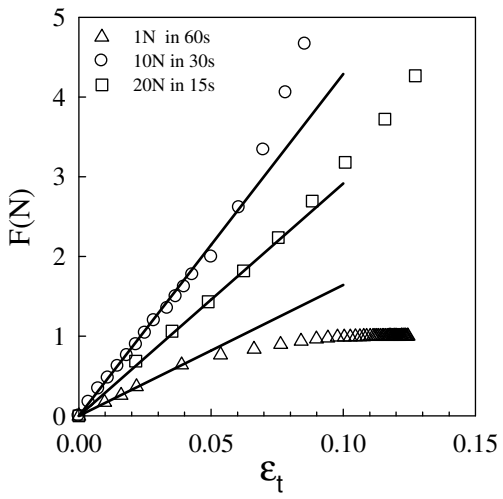


**Fig. 5**



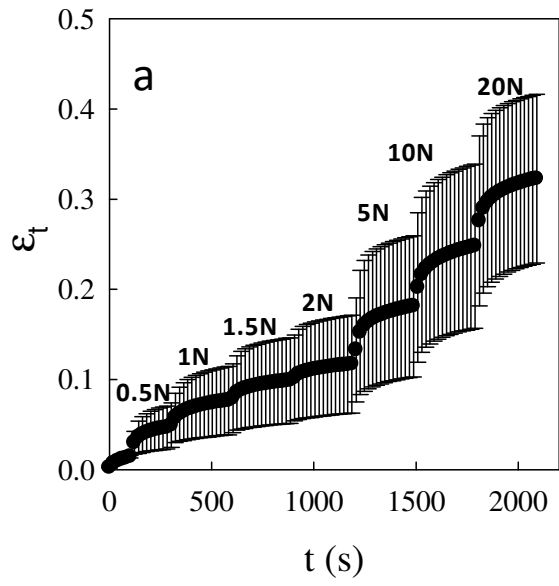


**Fig. 6a**

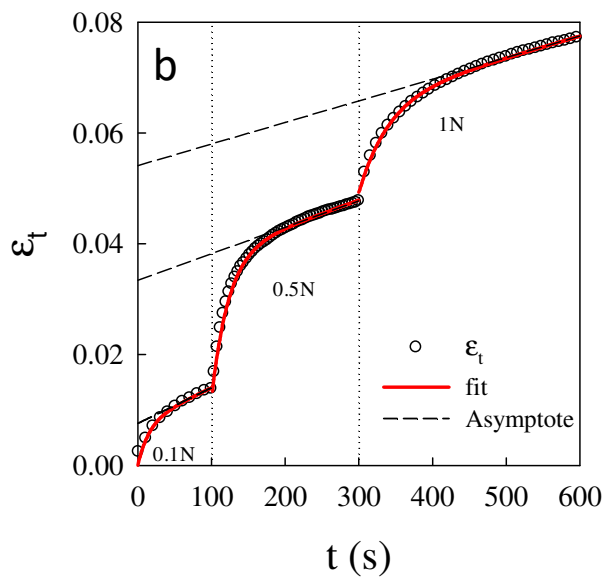


**Fig. 6b**

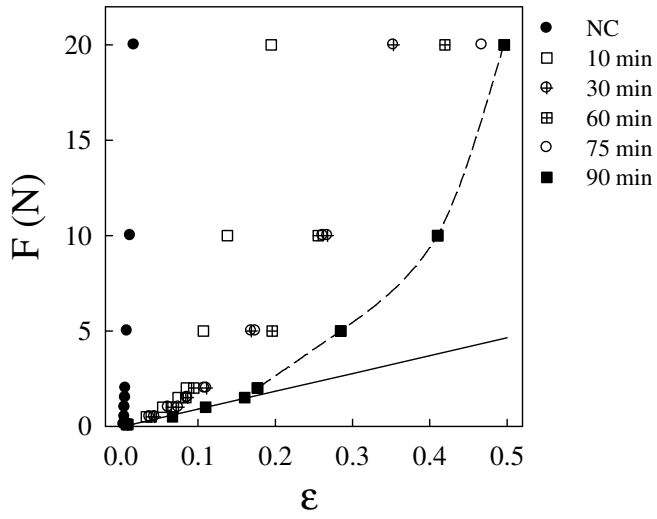


Fig. 7

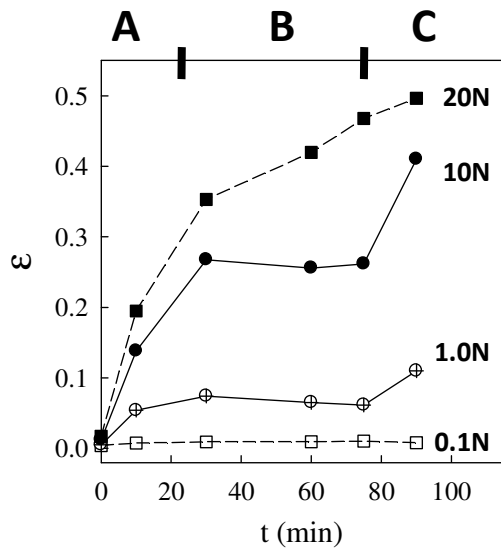
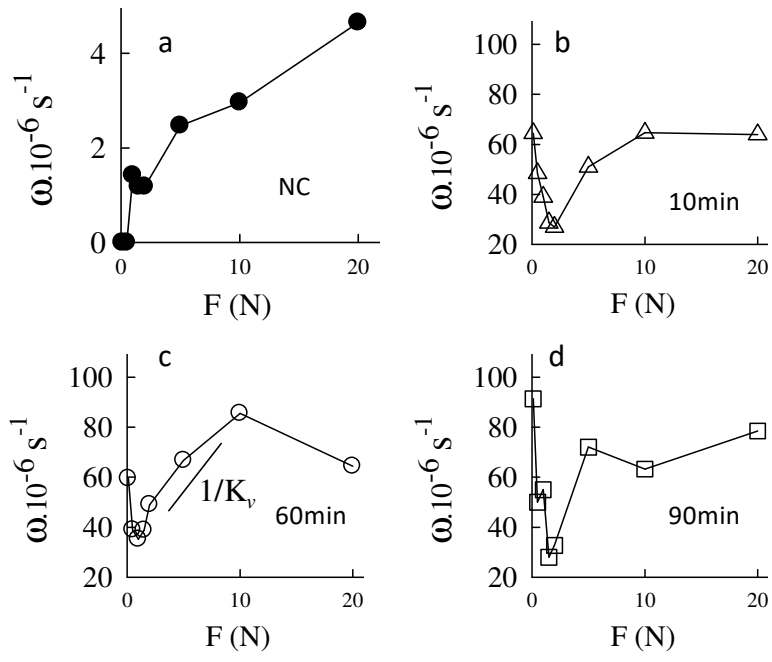
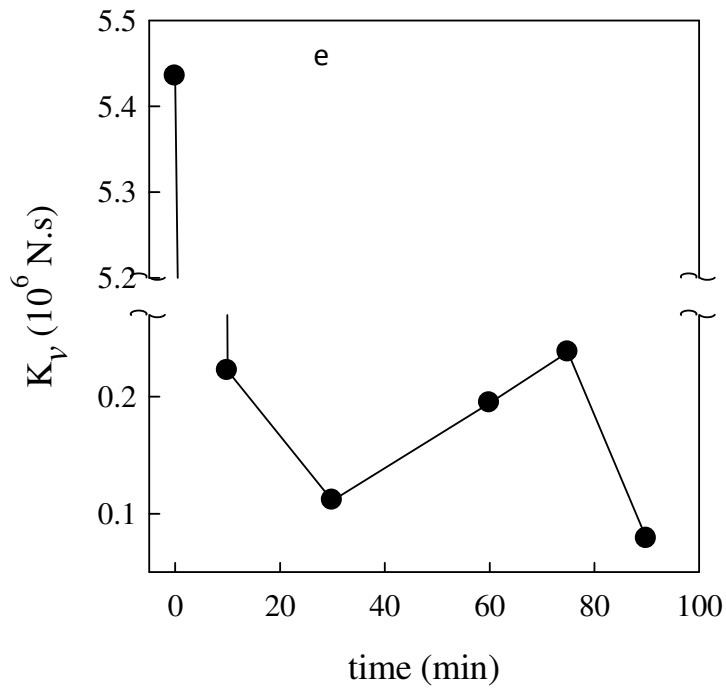


Fig. 8



**Fig. 9a, 9b, 9c, 9d**



**Fig. 9e**

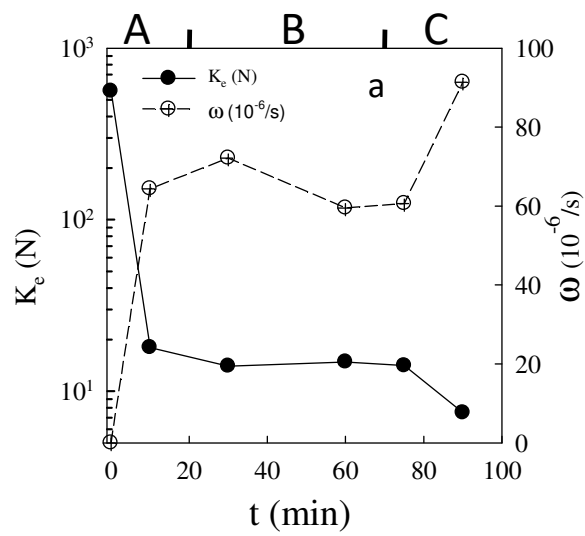


**Fig. 10a**

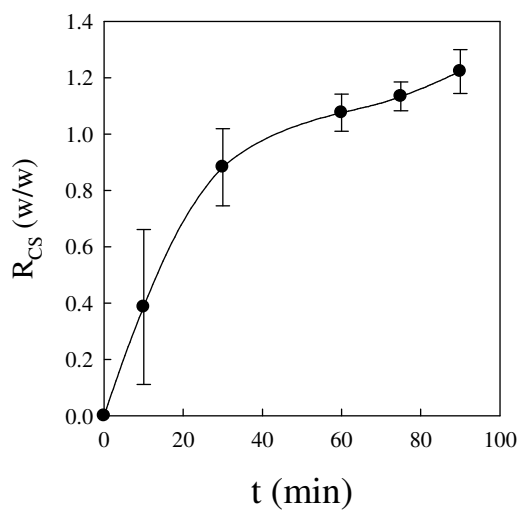


**Fig. 10b**

## Figure captions

*Fig.1: A) Picture of a native black eye cowpea seed; and the seed after having been simmered for B) 60min, C) 90min in the water at 95 °C and D) shows the finger test applied on the seed of C).*

*Fig.2: Picture of the experimental instrument (a) to show the onset of the compressive test (b) and the deformation of the seed under the compression (c)*

*Fig.3: a) Initial height position detection test repeated 3 times (open circle, square and diamond) shown as time dependence of the force during the course of the geometry toward the surface of the sample. The surface is detected when the force reaches 0.025N. b) Multiple step force program of the compression test, the insert shows the long-time compression test program for  $F = 1\text{ N}$ .*

*Fig. 4: Time-dependence of deformation  $\varepsilon_t$  of a cowpea seed after heating the seed at 95 °C for 10 min as a result of loading 1 N force (insert). The vertical dash line is the time where the force is reached. The continuous line through the data is the fit to equation (1) with  $\omega$  the slope of the dash line like the asymptote of the creep evolution ( $\omega t^\beta + \varepsilon$ ), and  $\varepsilon$  is where the asymptote crosses the time 0 axis. The fit parameters are:  $t_c = 23\text{ s}$ ,  $\alpha = 0.35$ ,  $\beta = 1$ ,  $\varepsilon = 7.13\%$ ,  $\omega = 6.35 \times 10^{-6}\text{ s}^{-1}$ .*

*Fig. 5: Deformation dependence of loading forces on seeds after heating at 95 °C for 10 min. The forces and the times it takes to load the forces are indicated in the legend. The seeds respond elastically in the beginning of the loading force. The higher the force that is loading, the faster the loading process and the higher the elastic deformation domain. This observation reflects the impact of the loading rate on the compliance of the samples.*

Fig.6: a) Time-dependence of deformation  $\varepsilon_t$  of a cowpea seed after heating the seed at 95°C for 10 min as a result of loading multiple forces. The error bars are the standard deviation calculated on the average of 4 seeds. b) is the zoom in the 0.1 N, 0.5 N and 1 N to show the fit to equation (1) and the crossing point of the asymptote with the time 0 axis. For the error bars of Fig. 6b see Fig. 6a or apply  $30\% \times \varepsilon_t$  to get the standard deviation.

Fig.7: Applied forces as function of the deformation  $\varepsilon$  for the native cowpea seed (NC) and the different times of heating the seeds at 95 °C. The full line through the data shows the elastic domain for the seeds after heating at 95 °C for 10 min and the slope reflects the elastic constant in N unit. The dash line is a guide for eyes. Apply  $30\% \times \varepsilon$  for horizontal standard deviation.

Fig.8: The deformation of the Fig. 7 is plotted as a function of the heating time at 95 °C when the forces indicated in the figure are applied. The finger test A, B, and C on the top axis represent how the cowpea seed was perceived by different people where A = Uncooked or not edible; B = cooked a little like firm on teeth, i.e. "al-dente"; C = cooked or well done. Apply  $30\% \times \varepsilon$  for vertical standard deviation and  $\pm 3$  min for horizontal (time) error bars.

Fig.9: Force-dependence of deformation,  $\omega$ , of native cowpea (a), heating times in the figures (b,c,d) at 95 °C reflect the evolution of the seeds viscosity ( $K_v$  in N.s unit) as a function of the heating time, time 0 is NC, (e).  $K_v$  is given by considering  $\omega$  as linear with  $F$  in the increasing (jamming) domain. Note that the break on the y-axis shows the amplitude of the loss of the  $K_v$  of the cowpea once it starts to cook and the time domain where  $K_v$  increases and this shows the transitioning between uncooked and cooked state. Apply  $30\% \times (K_v, \omega)$  for vertical standard deviation and  $\pm 3$  min for horizontal (time) error bars.

Fig.10: (a) Evolution of the elasticity constant,  $K_e$  on the left axis, and the deformation rate ( $\omega$ ) on the right axis for 0.1 N as a function of the heating time of the seed at 95 °C. Apply 30

$\% \times (K_e, \omega)$  for vertical standard deviation and  $\pm 3$  min for horizontal (time) error bars. (b)

Water uptake in w/w of cowpea seeds as function of the heating time at 95 °C. Error bars are  $\pm$  the standard deviation computed on 4 seeds for each heating time.

